Adsorption of Aryl Azothieno [2,3-*b*]pyridine Dyes on Corncobs

Remon M. Zaki[1], Ahmed S. A. Ibrahim*[2], Gamal A. Ahmed[1], Gehan A. A. Micky[3], Rasha H. Ahmed[3], and Adel M. Kamal El-Dean[1]

[1]Chemistry Department, Faculty of Science, Assiut University, Assiut 71516, Egypt, [2] Sugar Technology Department, Faculty of Sugar and Integrated Industries, Technology, Assiut University, Assiut 71515, Egypt and [3]Chemistry Department, Girls Faculty of Science, Al Azhar University, Egypt

Abstract

*Nowadays, water pollution is considered one of the most global unwanted environmental problems, so its treatment is of great importance. In this study, Corncobs, which are considered agro-cellulosic wastes, were used as highly efficient and low-cost sorbents for the adsorptive removal of some 4,6-dimethyl-2-(aryldiazenyl) thieno [2,3-b] pyridine-3(2H)-one dyes from aqueous solutions. The influences of the different operating parameters such as solution pH, sorbent dose, dye concentration, particle size, and contact time are extensively examined. From the experimental results, we found that the adsorption capacity attained its highest value at pH 12 and particle size 0.125 mm, also the adsorption reached equilibrium after 90 minutes. Results revealed that the adsorption data is well described by Langmuir and Freundlich isotherms with higher values of maximum adsorption capacities. It was found that the kinetic model for **Ia**, **Ic** and **Id** are consistent with a pseudo-second-order ($R^2 > 0.99$) and **Ib** is consistent with a pseudo–first-order ($R^2 > 0.99$). Therefore, kinetic studies demonstrated that the adsorption process is well fitted by pseudo-second-order model and ruled by pore diffusion and film diffusion mechanism.*

1. Introduction

Dyes are widely used in several industries such as plastic, textiles, food, paper, and cosmetics for coloring their products. However, it is annually estimated that about 10^5 commercially accessible dyes are used in the manufacture of about 7×10^4 tons of numerous coloring [1]. These industries are textile, dyeing, paper & pulp, paint & tannery, and dyes manufacture which contribute to environmental pollution by 54, 21, 10, 8 and 7%, respectively [2]. Depending on their molecular structures, synthetic dyes can be classified into different classes: (i) basic dyes or cationic dyes, (ii) acid dyes, (iii) direct dyes, (iv) disperse dyes, (v) reactive dyes, and (vi) vat dyes [2,3]. Additionally, rayon fibers and mordant dyes are examples of water-soluble dyes while vat, disperse and azo dyes are examples of non-soluble dyes [5]. Among all of these dyes azo dye is the most frequently used with an annual production rate of 70% [6]. However, all synthetic dyes are hazardous materials [7]. Thus, these harmful dyes should not be allowed to blend with water sources which may cause grave concerns to all water consumers lives, especially humans. Therefore, great efforts have been made to remove these dyes from the wastewater [8].

To minimize the possible danger to people and the environment, the literature survey provided several methods for eliminating these dyes from industrial wastewater so that these wastewater could be recovered and safely reused. Methods of dye remediation can be classified into three categories namely chemical, physical, and biological treatments [9]. Therefore, as alternative methods, physical

---

methods include adsorption on natural bio-sorbents, which are now highly interested in removing dyes from waste effluents [10], [11]. Adsorption is a widely utilized green separation process because of its simple implementation, low cost, ease of maintenance, and outstanding efficiency [11]. In this technique, several studies have used natural materials locally available, renewable, and of low cost [12]. The most popular and suggested method for treating wastewater in industries is activated carbon adsorption [13]. Even with its efficiency, activated carbon is still a costly, mostly imported substance. For this reason, it is essential to conduct research and development on novel naturally occurring, abundant, economically viable, and efficient adsorbents for the remediation of ecosystems [14]. New environmental protection requirements have surfaced recently, namely about the recycling and depollution of heavy metals, which call for environmentally acceptable depollution techniques [13], [15]. Bio-adsorbents such as biomass, agricultural solid waste, and modified or unmodified clays have shown promising results for the adsorption of pollutants [10], [16].

Among these sorbents are bagasse, coir pith, wheat straw, rice husk, pine sawdust, peanut hull, coffee husk, corncobs, orange peel, sugarcane dust, and luffa fiber [17]. A fascinating agricultural waste that can be used as an adsorbent is corncobs. Because of their extensive and abundant carbon content, corncobs have the potential to be a useful and accessible local resource for research. Since corncob's structural components include lignin (6%), hemicellulose (36%), and cellulose (41%) [18]. However, no research papers were seen in the literature concerning the utilization of corncobs in the adsorptive abstraction of azothieno [2,3-*b*] pyridine dyes. Thus, in the current study, the removal of the previously synthesized azothieno [2,3-*b*]pyridine dyes from aqueous solutions using corncobs was investigated. Several parameters such as pH, contact time, the particle size of adsorbents, and adsorption process isotherms have been studied. Kinetic studies of the adsorption of dyes on corncobs were also studied. The selection of corncobs for this study was based on their high abundance, low-cost raw material, and environmental impact. The equilibrium adsorption capacity of dyes on the corncob was determined using the *Freundlich* and *Langmuir* isotherm equations. Furthermore, the adsorption kinetics of the dyes was studied by application of pseudo-first, second order, and intraparticle models.

2. Materials and methods
2.1. Preparation of Adsorbent
Corncobs were collected locally from Assiut governorate, Egypt, then crushed, washed, and dried at 80 °C for 5 h in a static air oven and finally sieved into different particle sizes ranging from 0.125 to 2 mm.

2.2. Chemicals
A fresh solution of sodium hydroxide (0.01 mol), purity ≥ 97 % was purchased from Piochem Egypt, and was used as a solvent in the adsorption study. *Aniline*, *p-chloroaniline*, *p-anisidine*, *p-nitroaniline*, and sodium nitrite with a purity of ~ 99% were purchased from SRL Chemicals India, and hydrochloric acid with a purity of 37% was purchased from Piochem Egypt. All these chemicals were used from their commercial sources and used without further purification.
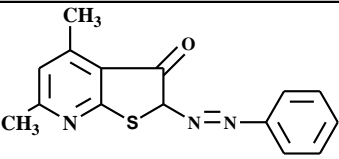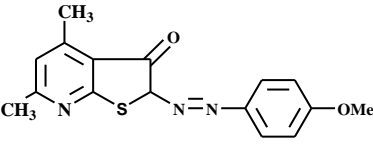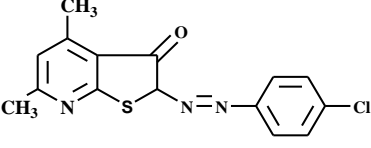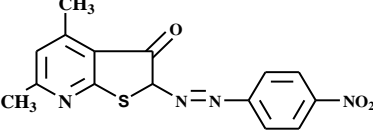
2.2 Dye (Adsorbate)
Azobenzene derivatives (a-d): Stock solutions (1 mmol/ dm^3) of the compounds were prepared by dissolving known weights of the dye in a definite volume of each solvent; then accurate dilution with the proper solvent was carried out. The pH control was achieved by using the modified universal buffer solutions [19].

2.3. Adsorption Technique
All of the sorption experiments were performed using the batch condition approach as performed in previous studies [20], [21]. A 100 mg L^{-1} stock solution of each dye was prepared, and the different

Table 1 Characterization of dyes Ia-d used in adsorption technique.

No	Chemical Structure	M.Wt.	Colour	λ_{max}
Ia		283.35	Dark red	487
Ib		313.37	Dark red	492
Ic		317.79	Dark red	494
Id		328.35	Violet	550

dye concentrations were diluted accordingly. **Adsorption equilibrium** experiments were carried out by adding 1.00 g of the dried adsorbent in 100 ml of dye solution with a desired concentration in a shaker [Hanaa model 211] at a constant speed (120 rpm) using a 250 ml conical flask containing the adsorbent for 2 h. At equilibrium, the adsorbent was separated from the solution by centrifuging or filtration through glass wool. the concentration of the remaining dye was spectrophotometrically determined using a UV–Visible spectrophotometer (EVOLUTION, model 300, England).

The pH values of the solutions were controlled using NaOH (0.1 M) and HCl (0.1 M). The quantity of dye sorbed, q_e (mg g^{-1}), and the percentage of dye removal were calculated by the following equations:

$$q_e = \frac{(C_0 - Ce)\, V}{w} \qquad (1)$$

Where C_0 and C_e are the initial and equilibrium concentrations of dyes, respectively (mg/L), V is the volume of the solution (L), and W is the weight of dry corncobs (g).

To assess the applicability of the adsorption process, it is necessary to determine the kinetic parameters, using the batch technique. A series of volumetric flasks containing 100 mL capacity were prepared, containing 50 mL dye solution of known concentrations at the appropriate pH and gaited by a mechanical shaker at room temperature (30 °C). After different time intervals, the solutions were filtered and then the filtrates were analyzed spectro-photometrically. All the experiments were duplicated and only the mean values are reported.

3. Results and discussion
3.1 Calibration curve for investigated dyes
The molar extinction coefficient (ε) of each dye was determined using Beers-Lambert relationship (C_0 versus Absorbance). The obtained results for the molar extinction coefficients (ε) of studied dyes are listed in **Table 2**.

Table 2 Molar extinction coefficients of the dyes under investigation.

Dye	ε (L mg^{-1} cm^{-1})	R^2
Ia	0.072	0.9993
Ib	0.071	0.9993
Ic	0.080	0.9991
Id	0.090	0.9992

3.2. Effect of contact time

The effect of contact time on the removal percentage of dyes is presented in **Fig. 1a**. The result revealed that the removal of the investigated dyes exhibited almost the same trend where it increased with increasing contact time to attain equilibrium at about 90-120 min. The plots represented the percentage removal of dyes versus the contact time for the (0.01 M) initial dye. The plots also revealed that the maximum percentage removal of dye was attained after 90 mins. of contact time. So, further experiments were conducted at 180 mins. of contact. In addition, the values of % dye removal take the following order Id > Ib > Ic > Ia. Also, curves are single, smooth, and continuous until reaching saturation and suggesting possible monolayer coverage of both dyes on the surface of corncobs [22]. The first rapid dye removal can be rationalized as a rapid attachment of dyes Ia-d to the bio-sorbent surface or due to the large number of vacant sites available at the initial stage.

3.3. Effect of adsorbent particle size

The influence of particle size furnished important information for achieving the optimum dose of absorbent. As informed from the literature, the adsorption capacity is directly proportional to the total exposed surface and inversely to the particle diameter for non-porous adsorbents. The presence of many small particles provided an increase in adsorption with a greater surface area available for dye removal [23]. **Fig. 1b** shows the effect of corncob particle size on the percentage removal of dyes. In each study, 1 g of adsorbent in 100 ml NaOH solution of 32 mg L^{-1} of dye at an equilibrium time of 120 min. Results–showed that as the corncob particle size decreased, an increase in dye removal percentage was observed. such behavior may be attributed to the great accessibility to pores and the greater surface area for bulk adsorption per unit mass of the adsorbent.

3.4 The effect of pH

One of the most significant factors that affect the adsorption capacity of adsorbent is the solution pH. It was found that the sorption efficiency mainly depends on the solution pH where varying the pH of the solution leads to the variation in (i) the degree of ionization of the adsorbate, (ii) the extent of dissociation of the function groups on the active site of the sorbent, and (iii) the texture properties of adsorbent [24]. The impact of solution pH on the adsorption efficiency of corncob towards Azobenzene derivatives (a-d) dyes was examined in a range of pHs from 5 to 12 and the results are shown in **Fig. 1c**. These results clearly revealed that increasing the value of pH the removal percentage of dyes increased, thus, pH 12 is the optimum value for adsorption, where the isotherm models study were performed. Such results can be justified on the bases that at lower pH values, the functional OH$^-$ groups on the corncob surface are protonated to be OH$_2^+$ which eventually repulse with N$^+$ groups of the dyes and hence % removal will decrease. While increasing the solution pH, functional groups will be O$^-$ which will attract the N$^+$ and S groups of dyes and thus increase the % removal.

3.5. Adsorption isotherms

The equilibrium adsorption isotherms are one of the most important data for understanding the mechanism of the adsorption system which are fundamental in describing the interaction behaviors between solutes and adsorbents [25]. **Fig. 2** shows the variation of sorption capacity as mg of dye
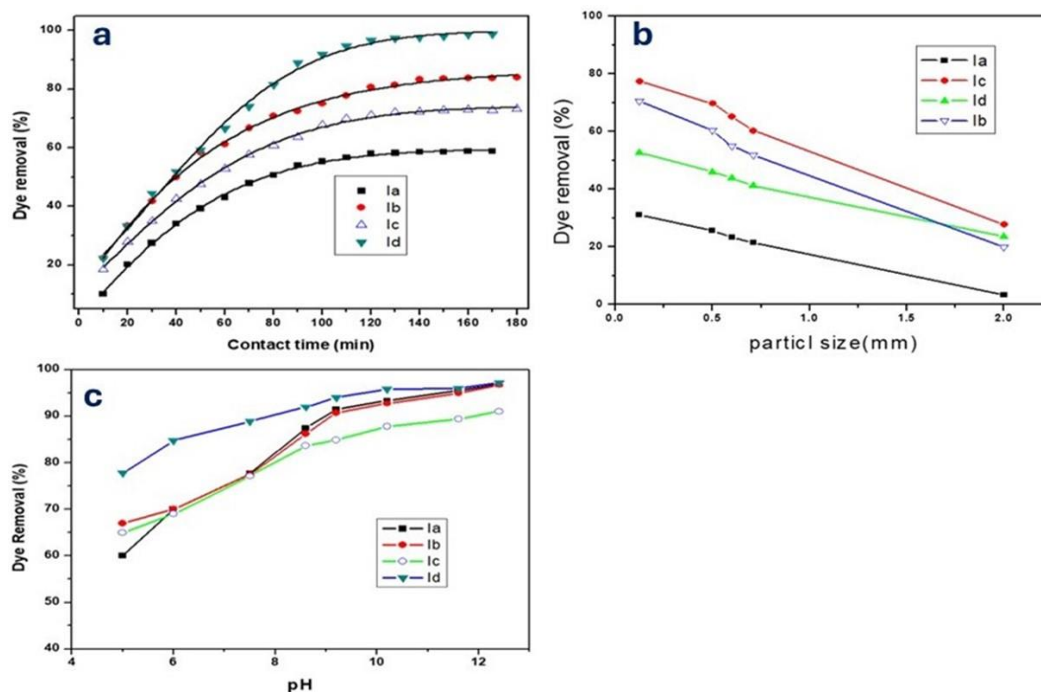
Fig. 1 a. Effect of contact time on adsorption of dye solution on Corncob, b. effect of sorbent particle size on dye removal, and c. effect of pH on adsorption of **Ia-d** dyes in 100 mg L^{-1} at a dose of 1.0 g of corncob, λ_{max}= 487 (**Ia**), 492 (**Ib**), 494 (**Ic**), and 550 (**Id**).

sorbed on 1.0 gm of corncob versus the initial concentration (Ce) of the different dyes **Ia-d** (Q_e). Results demonstrated that, as the dye concentration increases, the sorption capacity increases and attains equilibrium at a certain concentration. This may be a result of increasing the driving force of the concentration gradient with the increase in the amount of initial dye. Equilibrium isotherm equations are used to describe experimental adsorption data. The parameters obtained from the different models provide important information of the adsorption mechanisms, surface properties, and affinities of the corncobs. The most accepted surface adsorption models for single state systems are the *Langmuir* and *Freundlich* models.

3.5.1. Langmuir isotherm

The *Langmuir* isotherm theory assumed monolayer coverage of adsorbent over a homogenous adsorbent surface [26]. A basic assumption is that adsorption took place at specific homogeneous sites within the adsorbent. Once a dye molecule occupies a site, no further adsorption can take place at this site. The following equation represents the *Langmuir* isotherm, equation:

$$Ce \ / \ Qe = 1/ \ Q_ob + (\ 1/Qo)Ce \qquad (2)$$

where Ce is the equilibrium concentration (mg/ L), Qe is the amount adsorbed at equilibrium (mg/g), and Q_0, b are *Langmuir* constants related to adsorption capacity (mg/g) and energy of adsorption (L/g) respectively. The linear plots of Ce/ Qe vs. Ce. **Fig. 3** showed that the adsorption obeyed *Langmuir* isotherm model for all dyes. The values of Q_0 and b were determined for each dye from intercept and slopes as shown in **Table 4**. The essential characteristics of Langmuir dimensionless constant separation factor or equilibrium parameter, R_L, which is defined by the following equation [27]:

$$R_L = 1/1 + b \ C_0 \qquad (3)$$

where C_0 is the initial dye concentration, mg/L. The values of separation factor R_L indicated the nature of the adsorption process as given below in **Table 3**.
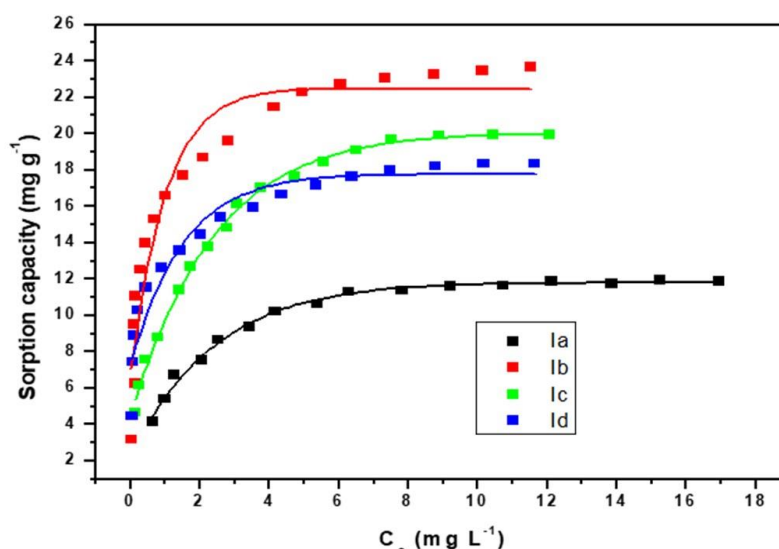
Fig 2: Adsorption isotherm of **a-d** dyes in 100 mg L^{-1} at a dose of corncobs = 1.0g of, contact time 90 mins, pH = 12, , λ_{max}= 487 (**Ia**), 492 (**Ib**), 494 (**Ic**), and 550 (**Id**).

Table 3 R_L value of Langmuire isotherm.

R_L value	Nature of the Process
$R_L > 1$	Unfavorable
$R_L = 1$	Linear
$0 < R_L < 1$	Favorable
$R_L = 0$	Irreversible

The excellent fit of the experimental data to the calculated ones and the higher correlation coefficients (R^2) indicated the applicability of the Langmuir isotherm model for dye Ia (R^2=0.998), dye **Ib** (R^2=0.998), dye **Ic** (R^2=0.997), and dye **Id** (R^2=0.997).

It is noted that the calculated maximum adsorption capacity, Q_0 is in good agreement with its experimental values obtained from adsorption isotherm curves shown in **Fig. 3.** The favorability of the adsorption process was calculated from the dimensionless separation factor (R_L), which was found between 0 and 1 which confirmed the ongoing adsorption of dyes.

3.5.2. Freundlich Adsorption Isotherm

The *Freundlich* adsorption model stipulates that the ratio of the solute adsorbed to the solute concentration is a function of the solution. The empirical model was shown to be consistent with an exponential distribution of active centers, characteristic of heterogeneous surfaces. The amount of solute adsorbed, Q_e, is related to the equilibrium concentration of solute in solution, C_e, by the following *Freundlich* isotherm equation:

$$Q_e = K_F \, C_e^{1/n} \qquad (4)$$

This expression can be linearized to give the following equation:

$$\log Q_e = \log K_F + 1/n \log C_e \qquad (5)$$

where K_F and n are *Freundlich* constants for the system, related to the bonding energy. K_F can be defined as the adsorption or distribution coefficient and respects the quantity of dye adsorbed onto adsorbent for a unit equilibrium concentration (a measure of adsorption capacity, mg/g). The slope $1/n$, ranging between 0 and 1, is a measure of adsorption intensity or surface heterogeneity, becoming more heterogeneous as its value gets closer to zero [28].
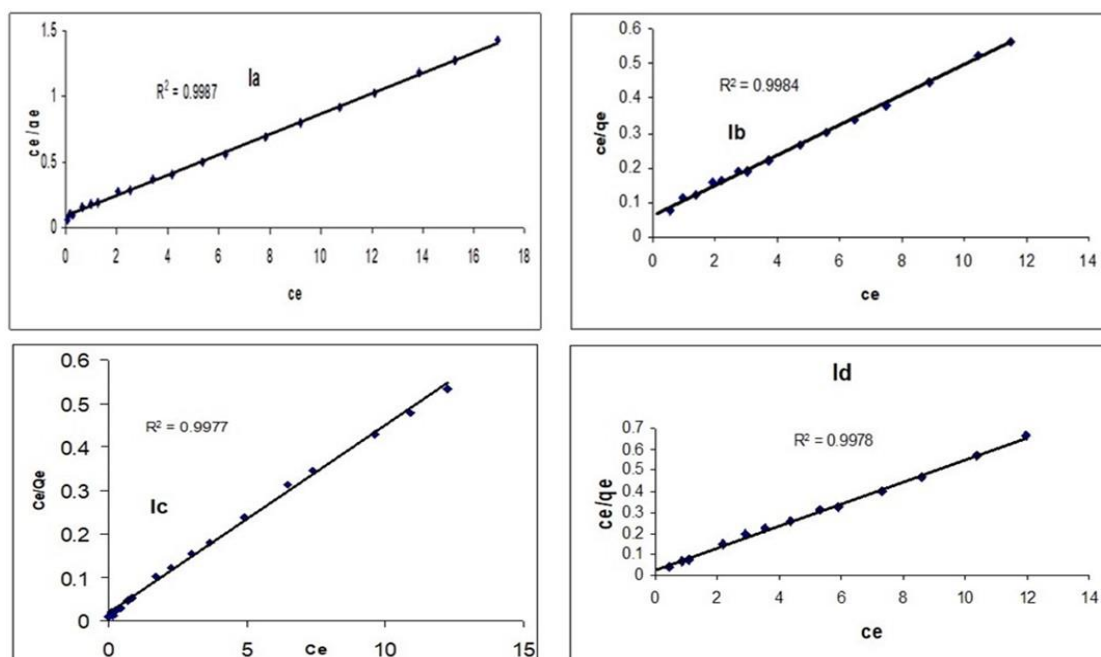
Fig. 3 *Langmuir* plots for the adsorption of compound **Ia-d** onto corncobs, at 1.0 g of corncobs, contact time = 90 mins, pH= 12, λ_{max}= 487 (**Ia**), 492 (**Ib**), 494 (**Ic**), and 550 (**Id**).

Table 4 *Langmuir* adsorption constant for of dyes Ia-d for different weights of Corncobs 1 g.

Dyes	Langmuir Isotherm			
	Q_0 (mg/g)	b	R^2	R_l
Ia	12.8	0.904	0.998	0.269
Ib	23.1	1.161	0.998	0.223
Ic	23.1	2.746	0.997	0.108
Id	19.0	3.246	0.997	0.093

The experimental data of *Freundlich* isotherm for the adsorption dyes **Ia-d** onto corncobs are represented in **Table 5** and **Fig. 4**.

The adsorption or distribution coefficient K_F, adsorption intensity or surface heterogeneity n, and the correlation coefficient (R^2) were calculated from the graphs represented in **Fig. 4** from intercept and slopes and the results were summarized in **Table 5**.

The distribution *coefficient* K_F increased with increasing the weight of corncobs. The slope $1/n$, ranging between 0 and 1, is a measure of adsorption intensity or surface heterogeneity, becoming more heterogeneous as its value gets closer to zero [28]. The correlation coefficients (R_F^2) of the Freundlich isotherm model for the phenyldiazenyl dye **Ia** was 0.895, for the *p*-anisyldiazenyl dye **Ib** was 0.985, for *p*-chlorophenyl diazenyl dye was **Ic** 0.971 and for *p*-nitrophenyl diazenyl dye **Id** was 0.997. These values obtained from adsorption isotherm curves are shown in **Fig. 4**.

From the previous results, we can conclude that the experimental data and the straight lines with Langmuir isotherm are better fitted correlation coefficients than in case of Freundlich isotherm confirming the homogeneous adsorption for dyes.

3.6. Adsorption Kinetic Study

To investigate the adsorption process of **Ia-d** dyes on corncobs, pseudo first order and pseudo second order were used. Pseudo first order and pseudo second order rate equations were expressed as follows:
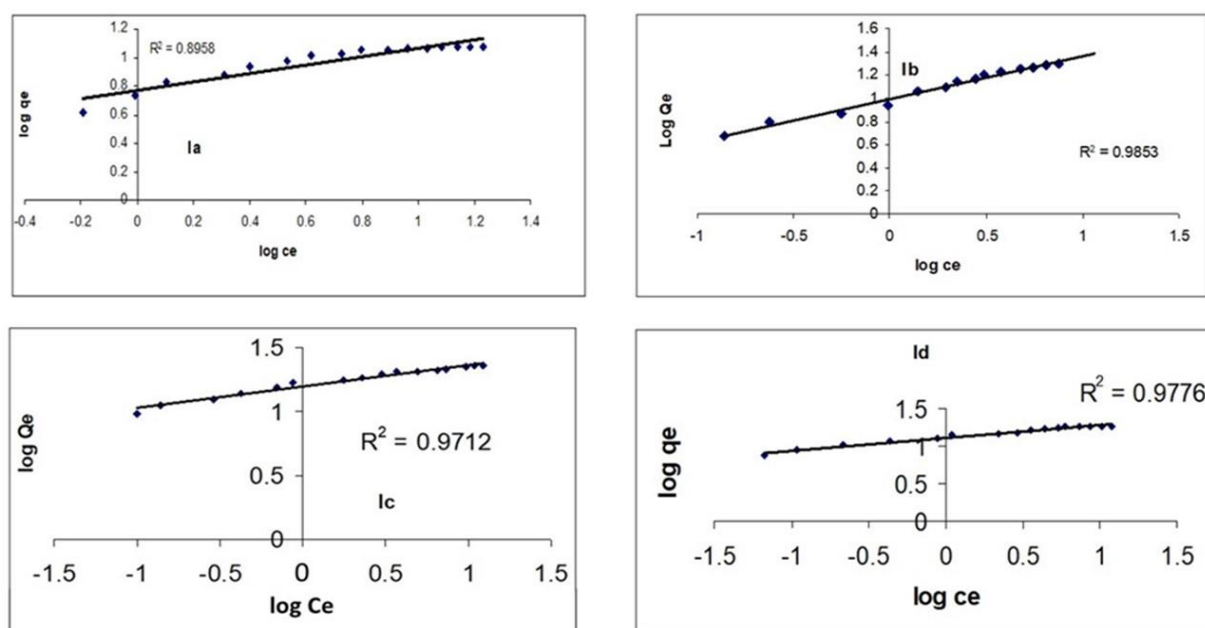
Fig. 4 *Freundlich* plots for the adsorption of dyes **Ia-d** at constant weight of corncobs 1.0 g, contact time = 90 mins, pH= 12, λ_{max}= 487 (**Ia**), 492 (**Ib**), 494 (**Ic**), and 550 (**Id**).

Table 5 *Freundlich* constant for the adsorption constant of dyes **Ia-d** at (1 g) of corncobs.

Dyes	Freundlich Adsorption Isotherm		
	K_F	n	R^2
Ia	11.94	3.40	0.895
Ib	9.79	2.87	0.956
Ic	15.63	5.88	0.971
Id	12.82	5.96	0.905

$$\text{Log } (q_e-q_t) = \text{Log } q_e - K_1 t/2.303 \qquad \text{pseudo-first-order} \qquad (6)$$

$$t/q_t = 1/h + t/q_e \qquad \text{pseudo-second-order} \qquad (7)$$

Where **q_e** and **q_t** are the amounts of adsorbed dyes (mg/ g) at equilibrium and at time t, respectively, K_1 is the rate constant of pseudo first order adsorption (min^{-1}), h $(K_2 q_e)^2$ is the initial adsorption rate (mg/g.min) and K_2 is the rate constant of pseudo second order adsorption (mg/g.min). The straight lines obtained and presented in **Fig. 5** indicated the applicability of the above equations. The values of K_1 and K_2 were calculated from the slopes of the respective linear plots and were noted in **Table 6**. Comparing the correlation coefficients of both equations, we found that the kinetic model for **Ia**, **Ic** and **Id** are consistent with a pseudo –second order ($R^2 > 0.99$) and **Ib** is consistent with a pseudo – firsr order ($R^2 > 0.99$).

3.6.1. Intra-particle Diffusion Study

Weber and Morris [27] found an empirical function relationship common to the most adsorption processes in which the uptake varies almost proportionally with $t^{1/2}$ as the following equation:

$$q_t = K_{id} t^{1/2} + C \qquad (8)$$

Where K_{id} is the intra-particle diffusion rate constant, q_t (mg/g) is the amount of dye adsorbed at time t (min). A plot of qt versus $t^{1/2}$ should be a straight line with a slope K_{id} and intercept C. Values
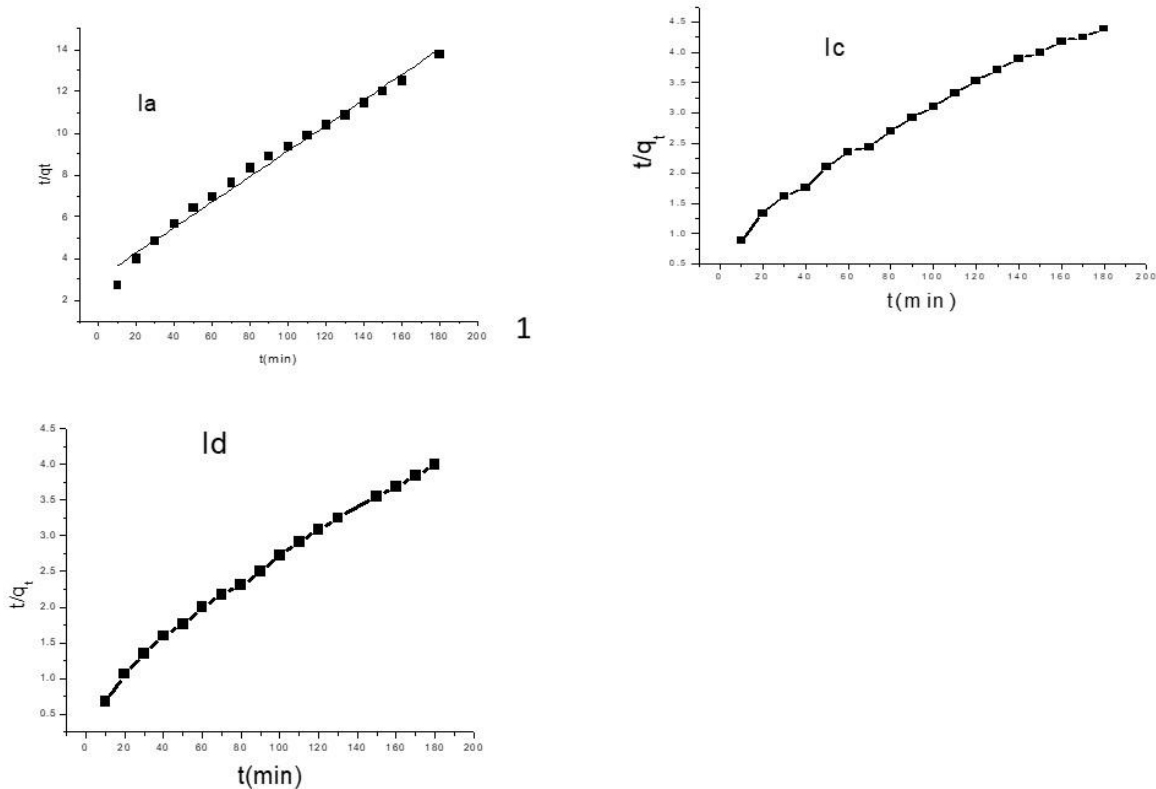
Fig. 5 The pseudo-second-order plot for **Ia**, **Ic**, and **Id** at constant weight of corncobs 1.0 g, contact time = 180 mins, pH= 12, λ_{max}= 487 (**Ia**), 494 (**Ic**), and 550 (**Id**).

Table 6 Comparison between the first and second-order adsorption rate constants *vs* the correlation coefficients

Dye	Pseudo first order		Pseudo second order	
	R^2	$k_1(min^{-1})$	R^2	$k_2 (mg\ g^{-1}min^{-1})$
Ia	0.996	0.0037	____	____
Ib	____	____	0.993	0.084
Ic	0.993	0.0049	____	____
Id	0.995	0.0048	____	____

of intercept give an idea about the thickness of the boundary layer, i.e., the larger the intercept the greater the boundary layer effect [29]. **Fig. 6** showed plots of the mass of dyes adsorbed q_t versus $t^{1/2}$ for (**Ia-d**) dyes. The results indicated that the adsorption process of both dyes exhibited separate regions with straight lines. The values of intercept, slope, and the correlation coefficient (R^2) were calculated and presented in **Table 7**. The deviation of the straight lines from the origin **Fig. 6** may be due to the difference in the rate of mass transfer in the initial and final stages of adsorption [29]. Furthermore, the first straight portion was attributed to a macropores diffusion process, and the second linear portion can be described as a micropore diffusion process [30]. Furthermore, the values of R^2 clearly proved the good applicability of the Weber-Morris equation [31]. The parameters of the intraparticle diffusion data for **Ia-d** dyes are listed in **Table 7**.

Table 7 Intra-particle diffusion model parameters for **Ia-d** dye.

Dye	R^2	Slop	Intercept
Ia	0.998	1.091	0.111
Ib	0.991	2.555	0.3597
Ic	0.990	2.798	3.646
Id	0.990	2.935	6.758
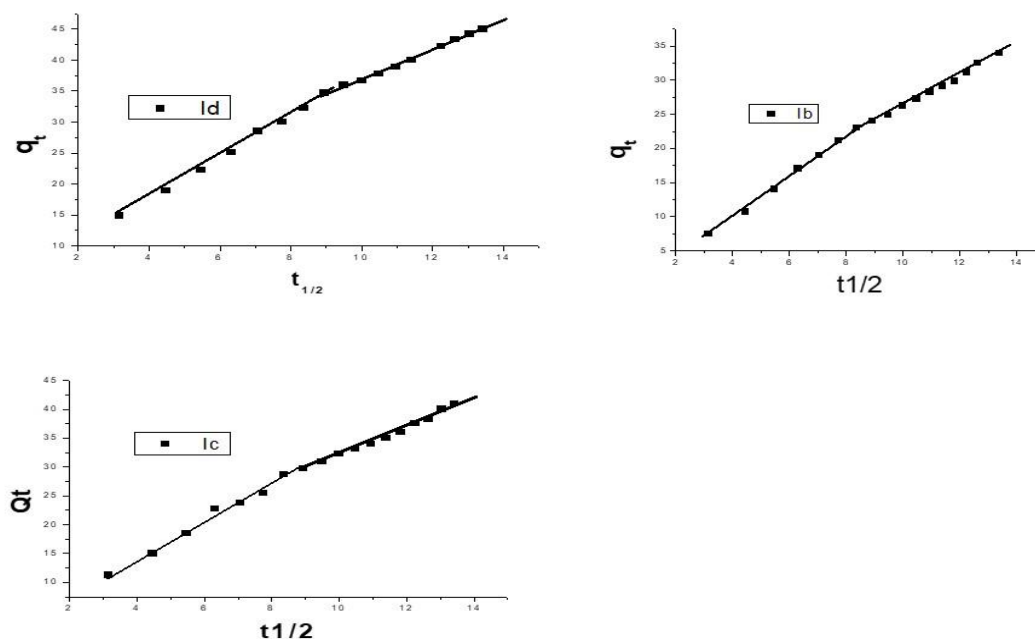
Fig. 6 Intra particle diffusion model for **Ib-d** at constant weight of corncobs 1.0 g, contact time = 180 mins, pH= 12, λ_{max}= 492 (**Ib**), 494 (**Ic**), and 550 (**Id**).

Conclusion

Low cost corncobs were prepared as adsorbent for the four prepared aryl thienopyridine dyes **Ia-d** from their aqueous solutions. Adsorbent doses and dye concentrations were varied. The adsorption capacities of corncobs increase in order a<d<b<c. The best adsorption capacity was determined at pH 12 and particle size of 0.125 mm, also the adsorption reached equilibrium after 90 minutes. The isotherm data could be well described by *Langmuir* and *Freundlich* equations in the dye concentration range from 1-31 mg/L. The *Langmuir* isotherm equation showed a somewhat better fit than the *Freundlich* isotherm.

References

[1] Katheresan, V., Kansedo, J., Lau, S. Y., Efficiency of various recent wastewater dye removal methods: A review. J Environ Chem Eng., 2018, vol. 6, pp. 4676–4697.

[2] Castillo-Suárez, L. A., Sierra-Sánchez, A. G., Linares-Hernández, I., Martínez-Miranda, V., and Teutli-Sequeira, E. A., A critical review of textile industry wastewater: green technologies for the removal of indigo dyes: Int. J of Enviro. Sci. and Technol., 2023, vol. 20, pp. 1-38.

[3] Salleh, M. A. M., Mahmoud, D. K., Karim, W. A. W. A., Idris, A., Cationic and anionic dye adsorption by agricultural solid wastes: A comprehensive review. Desalination., 2011, vol. 280, pp. 1–13.

[4] Chiou, M. S., Li, H. Y., Adsorption behavior of reactive dye in aqueous solution on chemical cross-linked chitosan beads. Chemosphere., 2003, vol. 50, pp. 1095–1105.

[5] Rauf, M. A., Salman Ashraf, S., Survey of recent trends in biochemically assisted degradation of dyes. Chemical Engineering Journal., 2012, vol. 209, pp. 520–530.

[6] Cotillas, S., Llanos, J., Cañizares, P., Clematis, D., Cerisola, G., Rodrigo, M. A., Panizza, M., Removal of Procion Red MX-5B dye from wastewater by conductive-diamond electrochemical oxidation. Electrochim Acta., 2018, vol. 263, pp. 1–7.

[7] Montoya-Suarez, S., Colpas-Castillo, F., Meza-Fuentes, E., Rodríguez-Ruiz, J., Fernandez-Maestre, R., Activated carbons from waste of oil-palm kernel shells, sawdust and tannery leather scraps and application to chromium(VI), phenol, and methylene blue dye adsorption. Water Science and Technology., 2016, vol. 73, pp. 21–27.

[8] Marcu, C., Varodi, C., Balla, A., Adsorption Kinetics of Chromium (VI) from Aqueous Solution Using an Anion Exchange Resin. Anal Lett., 2020, pp. 1–10.

[9] Amiralian, N., Mustapic, M., Hossain, M. S. A., Wang, C., Konarova, M., Tang, J., Na, J., Khan, A., Rowan, A., Magnetic nanocellulose: A potential material for removal of dye from water. J Hazard Mater., 2020, vol. 394, pp. 122571.

[10] Ibrahim, A. S., Gad, A. N., Dardeer, H. M., Gaber, A.-A. M., Chitosan-Cellulose Nanocomposite: Preparation, characterization, and evaluation as cationic color precipitant in sugar clarification process. Food Chem., 2023, pp. 135603.

[11] Ibrahim, A. S., Gad, A. N., Dardeer, H. M., Gaber, A.-A. M., Novel green biodegradable clarifying agents in sugar refining process using functionalized chitosan nanocomposites. Sustainable Materials and Technologies., 2022, pp. e00525.

[12] Aksu, Z., Isoglu, I. A., Use of agricultural waste sugar beet pulp for the removal of Gemazol turquoise blue-G reactive dye from aqueous solution. J Hazard Mater., 2006, vol. 137, pp. 418–430.

[13] Kali, A. et al., Characterization and adsorption capacity of four low-cost adsorbents based on coconut, almond, walnut, and peanut shells for copper removal. Biomass Convers Biorefin., 2024, vol. 14, pp. 3655–3666.

[14] Holliday, M. C., Parsons, D. R., and Zein, S. H., Agricultural Pea Waste as a Low-Cost Pollutant Biosorbent for Methylene Blue Removal: Adsorption Kinetics, Isotherm And Thermodynamic Studies, Biomass Convers Biorefin., 2024, vol. 14, pp. 6671–6685.

[15] Liu, Y., Li, X., Wang, Y., Zhou, J., and He, W., Preparation and characterization of Camellia oleifera nut shell-based bioadsorbent and its application for heavy metals removal, Bioresources., 2018, vol. 14, pp. 234–250.

[16] de Andrade Neto, J. C., Pereira, G. J., and Morandim-Giannetti, A. A., Chitosan and corn stover derivative bioadsorbent: characterization and application in hexavalent chromium adsorption processes, Cellulose., 2020, vol. 27, pp. 6317–6331.

[17] Mahmoodi, N. M., Arami, M., Bahrami, H., Khorramfar, S., Novel biosorbent (Canola hull): Surface characterization and dye removal ability at different cationic dye concentrations. Desalination., 2010, vol. 264, pp. 134–142.

[18] Haryanto, B., Tambun, R., Sinaga, R. F. J., Sembiring, S. V., Hutabarat, A., and Alexander, V., Comparison of natural corn cob and carbon corn cob in the purification of used cooking oil with shaker operation," IOP Conf Ser Earth Environ. Sci., 2024, vol. 1302, pp. 012066.

[19] Britton, H.T.S. Hydrogen ions. 2nd Edition, Chapman and Hall, London. 1952

[20] Abdel-Magied, A. F., Abdelhamid, H. N., Ashour, R. M., Zou, X., Forsberg, K., Hierarchical porous zeolitic imidazolate frameworks nanoparticles for efficient adsorption of rare-earth elements. Microporous and Mesoporous Materials., 2019, vol. 278, pp. 175–184.

[21] Malakootian, M., Hossaini, H., Asadipour, A., Daneshkhah, M., Preparation and characterization of modified sepiolite for the removal of Acid green 20 from aqueous solutions: isotherm, kinetic and process optimization. Appl Water Sci., 2018, vol. 8, pp. 1–12.

[22] Malik, P. K., Use of activated carbons prepared from sawdust and rice-husk for adsorption of acid dyes: a case study of Acid Yellow 36. Dyes and Pigments., 2003, vol. 56, pp. 239–249.

[23] Liew Abdullah, A. G., Salleh, M., Siti Mazlina, M. K., Megat, M. J., Noor, M., Osman, M. R., Wagiran, R., Sobri, S., AZO DYE REMOVAL BY ADSORPTION USING WASTE BIOMASS: SUGARCANE BAGASSE. International Journal of Engineering and Technology., 2005, vol. 2, pp. 8–13.

[24] Nandi, B. K., Goswami, A., Purkait, M. K., Removal of cationic dyes from aqueous solutions by kaolin: Kinetic and equilibrium studies. Appl Clay Sci., 2009, vol. 42, pp. 583–590.

[25] Özcan, T., Galil, B. S., Bakir, K., Katağan, T., The first record of the banana prawn Fenneropenaeus merguiensis (De Man, 1888) (Crustacea: Decapoda: Penaeidae) from the Mediterranean Sea. Aquat Invasions., 2006, vol. 1, pp. 286–288.

[26] Langmuir, I., The adsorption of gases on plane surfaces of glass, mica and platinum. J Am Chem Soc., 1918, vol. 40, pp. 1361–1403.

[27] WeberJr., W. J., Morris, J. C., Kinetics of Adsorption on Carbon from Solution. Journal of the Sanitary Engineering Division., 1963, vol. 89, pp. 31–59.

[28] Haghseresht, F., Lu, G. Q., Adsorption Characteristics of Phenolic Compounds onto Coal-Reject-Derived Adsorbents. Energy and Fuels., 1998, vol. 12, pp. 1100–1107.

[29] Kannan, N., Sundaram, M. M., Kinetics and mechanism of removal of methylene blue by adsorption on various carbons—a comparative study. Dyes and Pigments., 2001, vol. 51, pp. 25–40.

[30] Panday, K. K., Prasad, G., Singh, V. N., Mixed adsorbents for Cu(II) removal from aqueous solutions., 2008, vol. 7, pp. 547–554.

[31] Inbaraj, B., Sulochana, N., Basic dye adsorption on a low cost carbonaceous sorbent- Kinetic and equilibrium studies. Indian Journal of Chemical Technology., 2002, vol. 9, pp. 201-208.